JSEE
Journal of Sustainable Energy & Environment

Journal of Sustainable Energy & Environment

11 (2020) 1-10

# Impacts of transboundary smoke haze from biomass burning in lower Southeast Asia on air quality in Southern Thailand

Parisa Shokoohinia[1, 2], Nosha Assareh[1, 2], Kasemsan Manomaiphiboon[1, 2, *], Chatinai Chusai[3], Supachita Kerkkaiwan[1, 2], Kessinee Unapumnuk[4] and Nishit Aman[1, 2]

[1]The Joint Graduate School of Energy and Environment, King Mongkut's University of Technology Thonburi, Thailand
[2]Center of Excellence on Energy Technology and Environment, Ministry of Higher Education, Science, Research, and Innovation, Thailand
[3]Department of Primary Industries and Mines, Ministry of Industry, Thailand
[4]Air Quality and Noise Management Bureau, Pollution Control Department, Thailand
*Corresponding author: E-mail: kasemsan_m@jgsee.kmutt.ac.th, Tel.: +66 2 470-7331

**Abstract:** This study investigated the impact of transboundary smoke haze from Indonesia on air quality in Southern Thailand, with focus on Songkhla and Phuket provinces. Long-term $PM_{10}$ (particulate matter whose size is no larger than 10 μm) and visibility data were considered. It was found that elevated $PM_{10}$ tends to occur in the haze-prone period (May-November) and be more induced in strong El Nino years (here, 1997 and 2015), with $PM_{10}$ degradation at Songkhla being more pronounced than at Phuket. The seasonality of monthly mean $PM_{10}$ and $VIS_d$ is not as apparent as that of the high-end and low-end percentiles respectively, suggesting a high degree of episodicity for the $PM_{10}$ problem. Elevated $PM_{10}$ episodes at Songkhla and Phuket were identified by examining daily $PM_{10}$ time series. Kinematic back-trajectory results simulated for individual elevated $PM_{10}$ episodes during the haze-prone period (42 and 4 episodes at Songkhla and Phuket, respectively) show that the majority of the episodes (63% at Songkhla and 100% at Phuket) have back-trajectories passing over fire cluster(s) located in Sumatra or Borneo and often associated with the warm (El Nino) or neutral phases of the El Nino-Southern Oscillation or ENSO. This evidently affirms the potential transboundary smoke haze from biomass burning in Indonesia, which induces elevated $PM_{10}$ in Southern Thailand.

**Keywords:** Smoke haze, back-trajectory, $PM_{10}$ exceedance, biomass burning, El Nino.

## 1. Introduction

By definition, biomass burning is the combustion of organic matter (i.e. living and dead vegetation) in an open area [1]. It can cause serious environmental issues and is one of the significant air pollution sources with global, regional, and local impacts on air quality, public health, and climate [2]. Most biomass burning occurs in tropical regions where fires are used for different purposes such as agricultural land cleaning, deforestation, shifting cultivation, and energy production [3]. Southeast Asia is considered one of the heavily impacted regions by biomass burning, with several hectares of forests and vegetation burned annually by intentional fires [4]. Uncontrolled fires in Indonesia have significantly increased since 1980s and been substantially found in Sumatra and Borneo (or Kalimantan) Islands, especially their southern parts [5]. Since many parts of Indonesia are covered by peat swamp forests, and peat is sedentarily accumulated material consisting of at least 30% of total dry mass as dead organic materials which store plenty of semi-decomposed organic matters [6]. Fires, when occurring, can burn and last relatively long in time and then emit considerable particulate and gaseous air pollutants as well as greenhouse gases. Incomplete biomass burning produces toxic pollutants, especially hydrocarbons. Secondary particulate and gaseous pollutants can form from emitted precursors. Favorable meteorological conditions, in particular strong synoptic winds, may allow fine particulate matters and other non-short-lived pollutants to travel over far distances, here aggregately called "smoke haze" [6].

Local air quality in many downwind areas of Southeast Asian countries (Indonesia, Malaysia, Singapore, Brunei, southern Thailand, and some parts of Philippines) is thus unavoidably impacted by transboundary smoke haze from Indonesia, causing several environmental and health problems [7-10]. In Sumatra and Borneo Islands, biomass burning is relatively intense in the dry season (May-November, defined here as the haze-prone period or months), during which land clearing for the next cycle of farming and deforestation to increase agricultural lands and are prevalent. Less rain and higher temperature in the dry season are favorable to sustain and spread fires, in contrast with December-April (defined as the non-haze-prone period or months) when rain and moisture are abundant and fires occur much less. The climate or weather system of Sumatra and Borneo is generally governed by the monsoon, consisting of two phases: the wet season in January-March and the dry season in July–September [5, 11]. The inter-annual variability of climatic conditions in Southeast Asia is well known to be influenced by the El Nino-Southern Oscillation (ENSO), which is an important large-scale climatic mode [12]. Its three phases are warm (or El Nino), cold (or La Nina), and neutral. El Nino can enhance regional drought, biomass burning, and also smoke haze [2, 5].

Various studies investigated the impact of biomass burning in Indonesia on air quality of Southeast Asian countries [7, 9, 13-14]. Most focused on a single or few smoke haze. For Southern Thailand, such particular studies have still been limited but the smoke-haze problem has existed and of much concern [10]. Pentamwa and Oanh [8] investigated a short smoke haze episode in August 2005 for Southern Thailand using back-trajectory modeling. It is known that smoke haze from Indonesia occasionally causes air quality to deteriorate so that public health, tourism, off-shore fishery, and transportation (both land and sea

 

due to low visibility) are affected. For example, in June-October 2015, daily (24-hour average) $PM_{10}$ level exceeded the national standard of 120 µg $m^{-3}$ for a number of times in several areas of the region [15]. In this study, long-term air quality data in Southern Thailand were considered to investigate the impact and extent and transboundary smoke haze. We first looked at and described the severity of problem using basic statistics derived from observational data, and we applied a back-trajectory modeling approach to inspect air-mass pathways associated with elevated $PM_{10}$ episodes.

## 2. Study area

The focus of this study is air quality degradation in the southern region of Thailand due to transboundary smoke haze from Lower Southeast Asia, in particular Sumatra and Borneo of Indonesia (Figure 1). The southern region, as part of the Malay Peninsula, is geographically divided into the east-coast and west-coast sides by elongated mountain ridges approximately aligned in the north-south direction. Administratively, it has a total of 16 provinces: 10 on the east coast (Phetchaburi, Prachuap Khiri Khan, Chumphon, Surat Thani, Nakhon Si Thammarat, Phatthalung, Songkhla, Pattani, Yala, and Narathiwat) and the rest on the west coast (Ranong, Phang Nga, Krabi, Phuket, Trang and Satun). Songkhla and Phuket were representatively chosen for study. Both are the largest in the east and west coasts, respectively, in terms of urbanization and economic development, and also offer many tourist destinations for rich cultures, beaches, and other recreational activities. Each has an urbanized central core as a city. Given the region's long and surrounding coastlines, its general climate is considered maritime [16], as opposed to continental climate in the other parts of Thailand, and mainly regulated by two regional monsoons [17]. The southwest monsoon spans May-October (i.e., the wet season), bringing moist warm air from Indian Ocean and then rain.

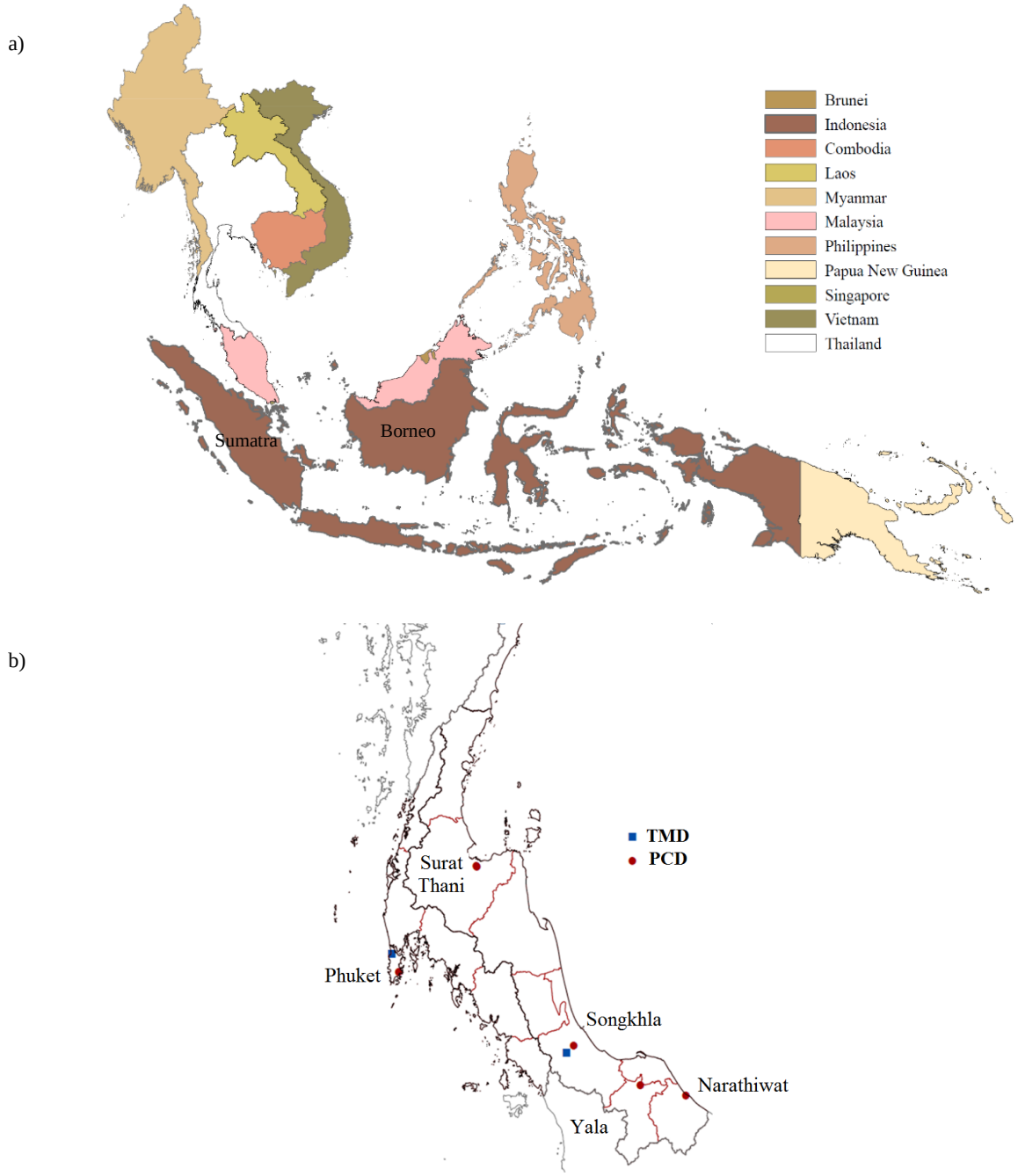


**Figure 1.** Maps of a) Southeast Asia, and b) Southern Thailand, showing the monitoring stations considered in the study.

The northeast monsoon is active in November and ends in February, bringing cool dry air from the mid-latitudes. As exception for November-January when the latter monsoon is quite intensified, air masses tend to pass through and absorb plenty of moisture from the Gulf of Thailand, resulting in substantial rain along the east-coast side of the region (Figure 2a). Monthly temperature in Songkhla and Phuket ranges between 27°C and 30°C, with the lowest and highest values in November-January and May, respectively. Local winds also link to the monsoons, and during the wet season, southerly and westerly winds are dominant for Songkhla and Phuket, respectively (Figure 3). The climate of Sumatra and Borneo has less seasonality [11], as compared to Southern Thailand. It is seen that most of the haze-prone months have apparently less rain, and May has the highest temperature (Figures 2c and 2d).

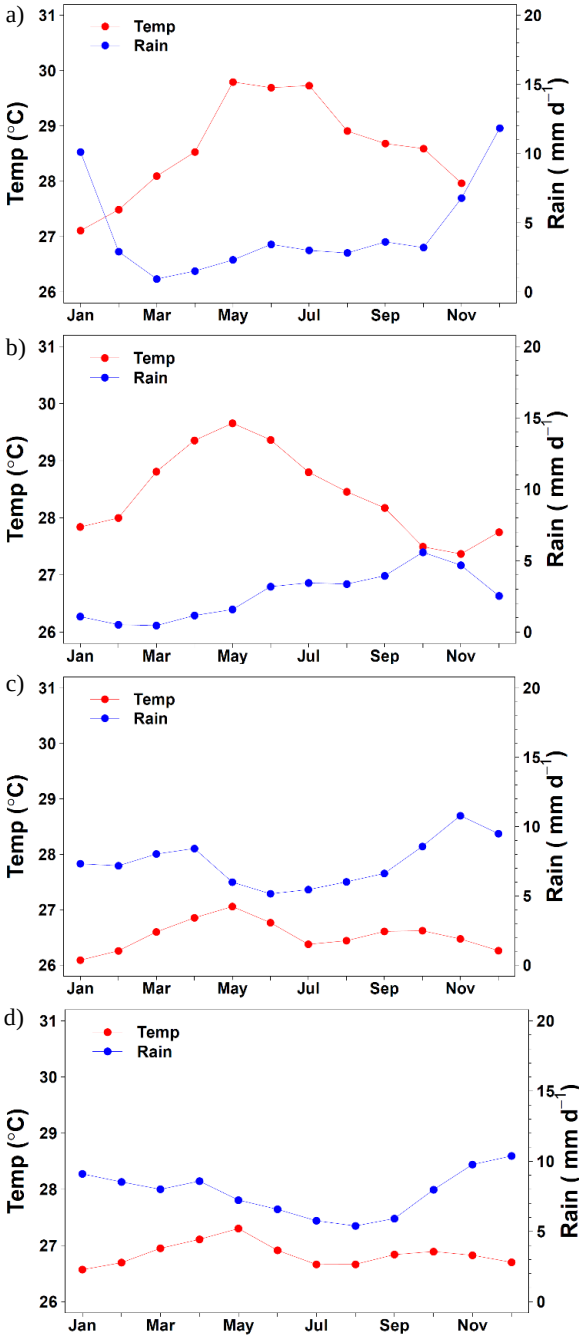


**Figure 2.** Monthly temperature and rain for a) Songkhla, b) Phuket, c) Sumatra, and d) Borneo.

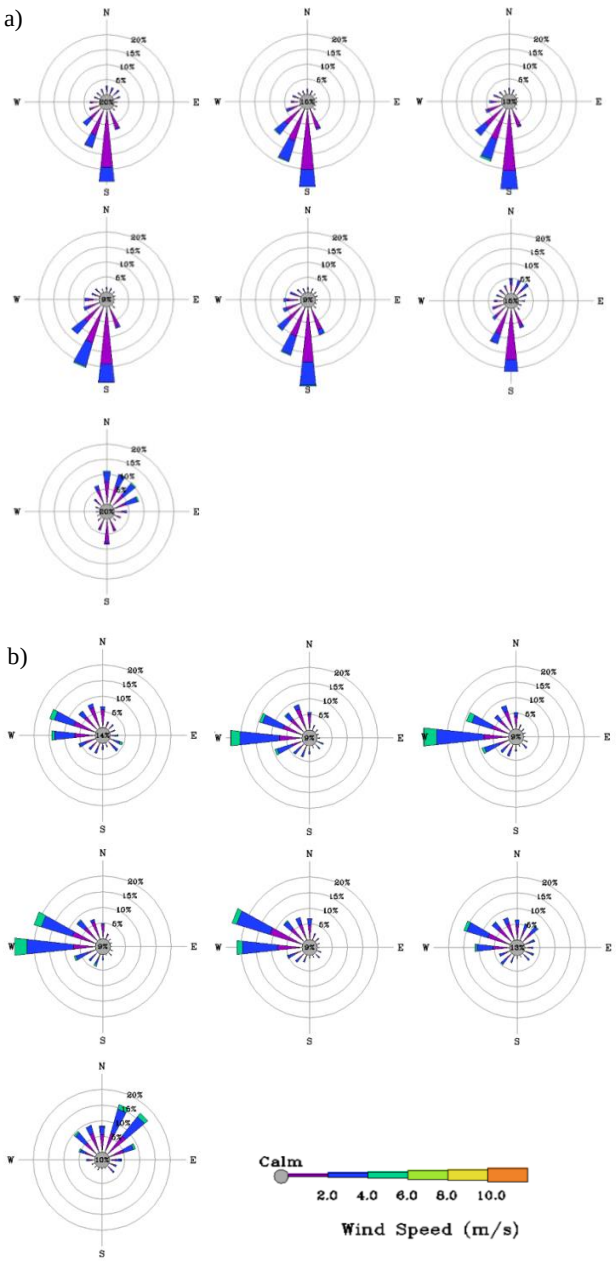


**Figure 3.** Monthly wind rose diagrams for May-November at a) Songkhla and b) Phuket.

### 3. Data and Methods

Hourly near-surface $PM_{10}$ data (measured at about 3 m agl or above ground level) at Songkhla and Phuket in the southern region were from the Pollution Control Department (PCD) of Thailand. The time coverage of the data is 1997-2016 (20 years) for Songkhla and 2008-2016 (9 years) for Phuket. We received supplementary $PM_{10}$ data for the following three provinces: Naratiwat (2006-2016), Yala (2006-2016), and Surat Thani (2004-2016) for. Along with hourly $PM_{10}$ are the following meteorological parameters: near-surface temperature, near-surface relative humidity, 10-m wind (speed and direction), and rain. Three-hourly daytime visibility data monitored by the TMD were also included (available at http://www.ncdc.noaa.gov). All initial data were quality checked, as summarized in Table 1. The amount of missing data was found to vary among the stations. Here, any variable with a large amount of missing data (here, >30%) was excluded. In general, the PCD

and TMD data used here have good adequacy with missing data being less than 20% for most of the available years. In our statistical calculation, at least 50% of all data values pooled must be present. Given that visibility is humidity-dependent, atmospheric aerosols can absorb humidity and then grow in size, leading to increase in light scattering, which thus reduces visibility [18]. As in Aman et al. (2019), the following relationship [19] was applied to adjust the original visibility to the non-humid or dry condition, which gives better representation for air pollution conditions:

$$\frac{\text{VIS}}{\text{VIS}_\text{d}} = 0.26 + 0.4285 \log_{10}(100 - \text{RH}) \quad (3.1)$$

where VIS is the original or initial visibility, $\text{VIS}_\text{d}$ is the RH-corrected visibility, and RH is the relative humidity (%). In the current analysis, a daily resolution was essentially considered. Daily conversion was conducted on hourly $PM_{10}$ as 24-hour average from 8 LT (local time) (the present day) to 7 LT (the next day) and for $\text{VIS}_\text{d}$ as the average of the values at 13LT and 16 LT [20].

Monthly 0.5° gridded data of the National Oceanic and Atmospheric Administration Climate Prediction Center (NOAA CPC) (available at ftp://ftp.cdc.noaa.gov/) were used to estimate temperature and rain over Sumatra and Borneo (as shown in Figures 2c and 2d). Monthly Oceanic Nino Index (ONI) was used to identify the El Nino, La Nina, and neutral phases (available at https://www.esrl.noaa.gov/). The index is three-month running averages of sea surface temperature anomalies over the tropical Pacific region of 5ºN-5ºS and 170ºW-120ºW (or the Nino 3.4 region). The ONI values from May to November in each calendar year were averaged to mark type of ENSO in that year (≥0.5°C as El Nino, ≤–0.5°C as La Nina, and otherwise, as neutral).

A smoke haze episode or event is identified by examining daily $PM_{10}$ time series. When $PM_{10}$ level goes up and start to cross the threshold of 60 μg $m^{-3}$, increases to 90 μg $m^{-3}$ or greater on later day(s), and finally decreases and reaches the 60 μg $m^{-3}$ threshold again, an episode is identified. The length of episode counts the number of days of from the two crossings while the duration of elevated $PM_{10}$ counts only those with 90 μg $m^{-3}$ or greater found in the episode. It is noted that the 60 μg $m^{-3}$ and 90 μg $m^{-3}$ levels correspond approximately to the 70$^{th}$ and 95$^{th}$ percentiles of daily $PM_{10}$ during the haze-prone period at Songkhla. Accordingly, 42 and 4 episodes were found for Songkhla and Phuket, respectively (see Tables 3 and 4).

Back-trajectory modeling was performed to assess the pathways of air masses associated with each smoke haze episode during the haze-prone period. FLEXTRA (version 5.0) [21] (available at http://flexpart.eu) was employed to simulate kinematic back-trajectories for each individual episode, which was set to travel backward in time for 8 days. The driving wind fields for the modeling is 6-hourly 0.5º Climate Forecast System Reanalysis (CFSR) data [22]. The arrival times of back-trajectory was set to 4 times a day (0, 6, 12, and 18 UTC; LT = UTC + 7). As for arrival height, several previous studies used a single height, e.g., 500 m agl. [23], which is applicable when considering the thickness of daytime ABL in the tropics being about 1-3 km. The early afternoon hour generally represents the time of strong convective mixing and the fairly-to-well developed atmospheric boundary layer (ABL). However, FLEXTRA offers several options to initialize back-trajectories, and one of them is coherent ensemble of trajectories (CET), which was used here. This mode initializes a number of starting points over a uniform three-dimensional grid and is thus suitable to investigate the potential air pollutant sources, as opposed to a single location or height. Here, at each of Songkhla, and Phuket, the CET domain includes 21 uniform vertical levels extended from the ground to 2 km, at each of which 3×3 uniform receptors are placed with a 0.25° spacing (i.e., 189 receptors in the CET domain). Assume that the length of a smoke haze episode is 8 days and the elevated $PM_{10}$ duration is 2 days, the total number of back-trajectories equals to 1,512 (= 189 CET receptors × 4 times $d^{-1}$ × 2 elevated $PM_{10}$ days).

To identify the potential sources of smoke haze from Indonesia, several trajectory-based methods have been used [20, 24-26]. In the current study, a simple technique was adopted here by visually examining the simulated back-trajectory pathways for an evidence of transboundary smoke haze from Sumatra or Borneo as the potential source areas if a non-trivial number of back-trajectories cross the target areas together with the presence of fire cluster(s) in each smoke haze episode.

An active fire data product (here, MCD14ML Collection 5) was used to indicate biomass burning occurrences or fires [27] (available at ftp://fuoco.geog.umd.edu/modis/). In this product, derived fire pixels have a resolution of 1 km based on the combined detection of the MODIS (Moderate Resolution Imaging Spectroradiometer) sensors aboard the Terra (launched in 1999) and Aqua (launched in 2002) satellites of the National Aeronautics and Space Administration (NASA). The data cover all years since 2000. In each episode, all MODIS-based fires were pooled from all elevated $PM_{10}$ days plus the previous 8 days of the first elevated day, mapped on the target areas, and then visually examined if any large fire cluster(s) are present.

**Table 1.** Suitable ranges and outliers of selected parameters.

| Parameter | Units | Suitable Range | Outlier |
|---|---|---|---|
| $PM_{10}$ | μg $m^{-3}$ | 0-600 | Mean ± 10·SD |
| VIS | km | ≥0 | Not applicable |
| Wind speed | m $s^{-1}$ | 0-50 | Mean ± 10·SD |
| Wind direction | degrees from north | 0-360 | Not applicable |
| Temperature | ºC | 5-50 | Not applicable |
| Relative humidity | % | 0-100 | Not applicable |
| Rain | mm $3h^{-1}$ | 0-300 | Mean ± 10·SD |

## 4. Results and Discussion

### 4.1 Severity of smoke haze

Monthly average $PM_{10}$ over 1997-2016 at the selected five stations in the southern region of Thailand show strong fluctuation year by year (Figure 4a). Most obviously, sharply elevated $PM_{10}$ at Songkhla tends to occur during the haze-prone period, and nearly all exceedances at all stations, if found, are present in the same period as well (Figure 4b), suggesting the air quality degradation being seasonal and due potentially to smoke haze.

Songkhla is the city with the most serious $PM_{10}$ problem, with as many as 20 exceedances in the haze-prone period over the 20-years, while Phuket has 5 exceedances based on the 9-year data (Table 1). In 2015, the problem is prevalent region-wide with exceedances found at every station (Figure 4b), and turns the most serious for $PM_{10}$ mean in the haze-prone period (Figures 5a and 5b). Visibility (specifically, $\text{VIS}_\text{d}$) can also be seriously impacted, e.g., as low as 0.3 km and 1.2 km at Songkhla and Phuket, respectively (Table 2). However, seasonal mean $PM_{10}$ and $\text{VIS}_\text{d}$ are not necessarily expected to be higher and lower in the haze-prone months as compared to the other months (Table 2), respectively.

Similar results can be seen in the annual cycle of $PM_{10}$, with relatively low variation (i.e., low seasonality) in mean but high at the high-end percentiles (here, 75$^{th}$ and maximum) (Figures 5c and 5d). This is generally because the smoke haze problem is highly episodic, i.e., lasting from 1-3 days mostly to multiple days (e.g., 4-6 days) for some cases (Table 3). As seen from the table, in the non-haze-prone period, only one exceedance was found in Songkhla, suggesting local emission sources to play a more important role and the particulate pollution in the regions to be mostly associated with the biomass burning in Indonesia in the haze-prone months instead (Figures 5a and 5b).

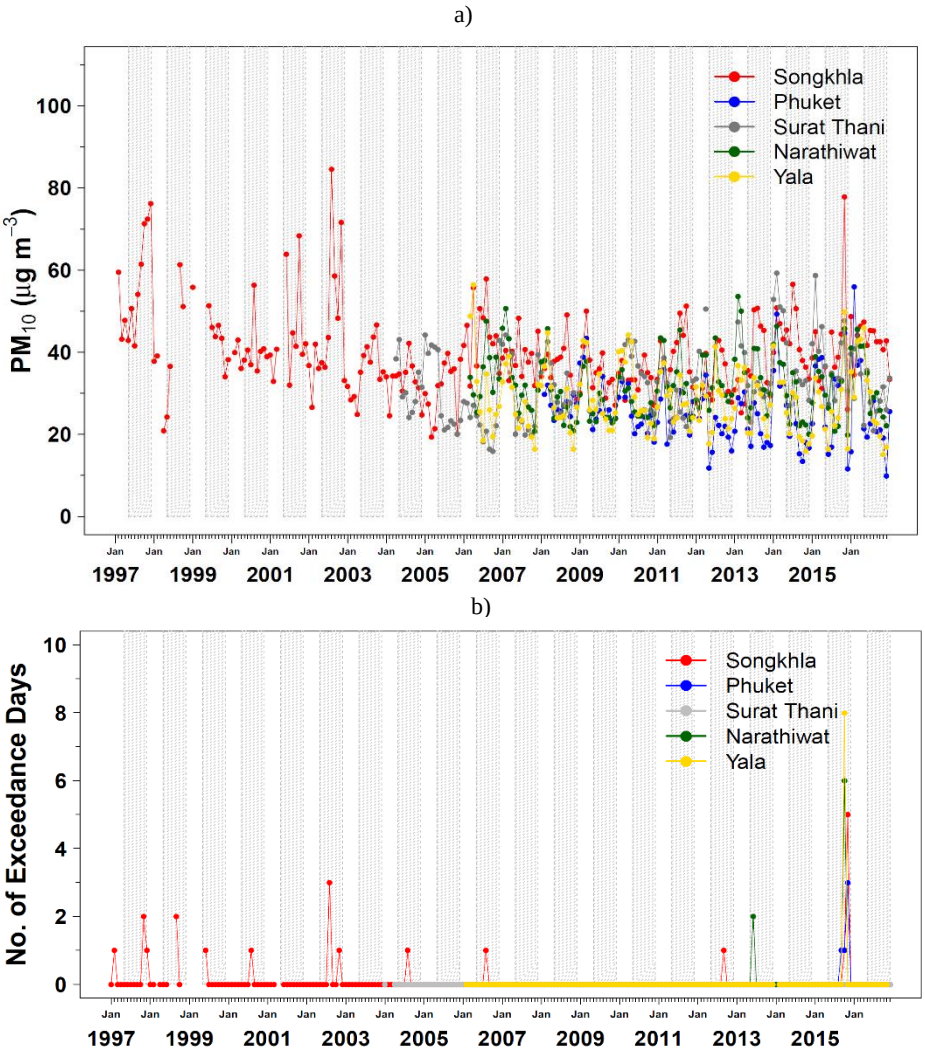


**Figure 4.** a) Monthly variation of $PM_{10}$ at the selected five stations in Southern Thailand, and b) monthly variation of $PM_{10}$ exceedance days at the same stations. The grey lines mark the haze-prone months (May-November).

**Table 2.** General statistics of 24-hour average $PM_{10}$ and daily daytime $VIS_d$ at Songkhla and Phuket.

| Statistic | Songkhla | | Phuket | |
|---|---|---|---|---|
| | **$PM_{10}$** (µg $m^{-3}$) | **$VIS_d$** (km) | **$PM_{10}$** (µg $m^{-3}$) | **$VIS_d$** (km) |
| **Haze-prone period** | | | | |
| Range | 9.9 to 291.8 | 0.3 to 21.1 | 4.8 to 202.4 | 1.2 to 13.0 |
| Mean ± SD | 41.4 ± 18.0 | 11.0 ± 1.7 | 23.0 ± 12.1 | 9.6 ± 1.7 |
| No. of exceedance days | 20 | Not applicable | 5 | Not applicable |
| **Non-haze-prone period** | | | | |
| Range | 5.0 to 123.9 | 1.3 to 15.9 | 6.1 to 84.1 | 3.5 to 12.1 |
| Mean ± SD | 36.6 ± 1 | 11.1 ±1.2 | 29.6 ± 12.2 | 9.5 ± 1.4 |
| No. of exceedance days | 1 | Not applicable | 0 | Not applicable |
| Remark: National daily (24-hour average) $PM_{10}$ standard = 120 µg $m^{-3}$ | | | | |

The annual cycle of $VIS_d$ is consistent with that of $PM_{10}$ (Figures 6a and 6b) at each of Songkhla and Phuket, with low monthly variation in terms of mean but more seasonality with relatively low in the haze-prone months as seen at the low-end percentiles (here, 25$^{th}$ and minimum). Moreover, most of low visibility values tend to occur in this period (Figure 6c). It should be noted that visibility at Phuket tends to be lower than that atSongkhla but they cannot be compared to each other because visibility monitoring is human-based using different or site-specific visibility target.

The high interannual variatio n of $PM_{10}$ during the haze-prone months is expected since transboundary smoke haze is generally controlled by the degree of biomass burning and weather pattern (Figure 7). The years 1997 and 2015 are distinct with relatively high $PM_{10}$ persistently over many haze-prone months, and both years have the strong El Nino phase associated with drastic drought and high temperature in Southeast Asia [12]. The highest-recorded daily $PM_{10}$ in Songkhla and Phuket commonly occurred in October 2015 at 291.8 µg $m^{-3}$ and 202.4 µg $m^{-3}$, respectively (see Figures 5c and 5d).

 

**Table 3.** Trajectory characteristics associated with the smoke haze episodes for Songkhla.

| No. | Start | End | Episode length (days) | Duration of elevated $PM_{10}$ (days) | ENSO type | Trajectories (%) passing over Sumatra or Borneo | Presence of fire cluster(s) |
|---|---|---|---|---|---|---|---|
| 1 | 1997-07-28 | 1997-07-30 | 3 | 1 | EL | 50.6 | - |
| 2 | 1997-08-04 | 1997-08-06 | 3 | 1 | EL | 39.5 | - |
| 3 | 1997-08-15 | 1997-08-17 | 3 | 1 | EL | 39.0 | - |
| 4 | 1997-08-19 | 1997-08-21 | 3 | 1 | EL | 61.7 | - |
| 5 | 1997-09-09 | 1997-09-11 | 3 | 1 | EL | 40.6 | - |
| 6 | 1997-09-12 | 1997-09-15 | 4 | 2 | EL | 66.9 | - |
| 7 | 1997-09-20 | 1997-09-27 | 8 | 5 | EL | 77.4 | - |
| 8 | 1997-09-28 | 1997-10-02 | 5 | 1 | EL | 52.7 | - |
| 9 | 1997-10-05 | 1997-10-07 | 3 | 1 | EL | 59.8 | - |
| 10 | 1997-10-11 | 1997-10-13 | 3 | 1 | EL | 60.3 | - |
| 11 | 1997-10-19 | 1997-10-21 | 3 | 1 | EL | 76.2 | - |
| 12 | 1997-10-26 | 1997-10-28 | 3 | 1 | EL | 0.5 | - |
| 13 | 1997-11-01 | 1997-11-04 | 4 | 2 | EL | 6.1 | - |
| 14 | 1997-11-06 | 1997-11-08 | 3 | 1 | EL | 1.2 | - |
| 15 | 1997-11-18 | 1997-11-23 | 6 | 2 | EL | 0.1 | - |
| 16 | 2000-07-10 | 2000-07-15 | 6 | 3 | LA | 19.1 | No |
| 17 | 2000-07-15 | 2000-07-19 | 5 | 2 | LA | 18.6 | No |
| 18 | 2001-09-07 | 2001-09-17 | 11 | 6 | N | 62.8 | No |
| 19 | 2002-07-10 | 2002-07-20 | 11 | 6 | EL | 30.6 | No |
| 20 | 2002-07-25 | 2002-07-29 | 5 | 1 | EL | 30.8 | No |
| 21 | 2002-08-22 | 2002-08-31 | 10 | 2 | EL | 18.5 | Yes |
| 22 | 2002-09-25 | 2000-09-27 | 3 | 1 | EL | 50.3 | Yes |
| 23 | 2002-10-07 | 2002-10-10 | 4 | 2 | EL | 2.1 | Yes |
| 24 | 2002-10-17 | 2002-10-22 | 6 | 2 | EL | 52.6 | Yes |
| 25 | 2003-08-21 | 2003-08-24 | 4 | 1 | N | 50.7 | Yes |
| 26 | 2003-09-10 | 2003-09-14 | 5 | 1 | N | 34.4 | Yes |
| 27 | 2004-07-10 | 2004-07-15 | 6 | 2 | N | 0.8 | No |
| 28 | 2005-08-12 | 2005-08-17 | 6 | 1 | N | 71.6 | Yes |
| 29 | 2005-11-12 | 2005-11-16 | 5 | 1 | N | 1.5 | No |
| 30 | 2006-0715 | 2006-07-19 | 5 | 3 | N | 40.0 | Yes |
| 31 | 2006-08-03 | 2006-08-07 | 5 | 1 | N | 42.1 | Yes |
| 32 | 2006-10-04 | 2006-10-10 | 7 | 1 | N | 51.9 | Yes |
| 33 | 2007-11-15 | 2007-11-27 | 13 | 1 | LA | 0.7 | No |
| 34 | 2008-07-27 | 2008-08-04 | 7 | 1 | N | 69.7 | No |
| 35 | 2011-09-05 | 2011-09-10 | 6 | 2 | LA | 36.7 | Yes |
| 36 | 2012-08-08 | 2012-08-14 | 5 | 2 | N | 45.1 | Yes |
| 37 | 2013-06-18 | 2013-06-25 | 8 | 2 | N | 33.4 | Yes |
| 38 | 2013-06-26 | 2013-06-29 | 4 | 1 | N | 1.5 | Yes |
| 39 | 2014-06-19 | 2014-06-24 | 6 | 1 | N | 3.0 | No |
| 40 | 2015-09-01 | 2015-09-04 | 4 | 1 | EL | 85.4 | Yes |
| 41 | 2015-10-02 | 2015-10-09 | 8 | 2 | EL | 68.5 | Yes |
| 42 | 2015-10-19 | 2015-10-26 | 8 | 3 | EL | 43.9 | Yes |

Remark:
-: No MODIS fire hotspot data

**Table 4.** Same as Table 3 but for Phuket.

| No. | Start | End | Episode length (days) | Duration of elevated $PM_{10}$ (days) | ENSO type | Trajectories (%) passing over Sumatra or Borneo | Presence of fire cluster(s) |
|---|---|---|---|---|---|---|---|
| 1 | 2015-08-25 | 2015-08-29 | 5 | 1 | EL | 83.3 | Yes |
| 2 | 2015-09-17 | 2015-09-23 | 7 | 3 | EL | 69.2 | Yes |
| 3 | 2015-10-02 | 2015-10-09 | 8 | 4 | EL | 55.3 | Yes |
| 4 | 2015-10-19 | 2015-10-22 | 4 | 1 | EL | 7.2 | Yes |

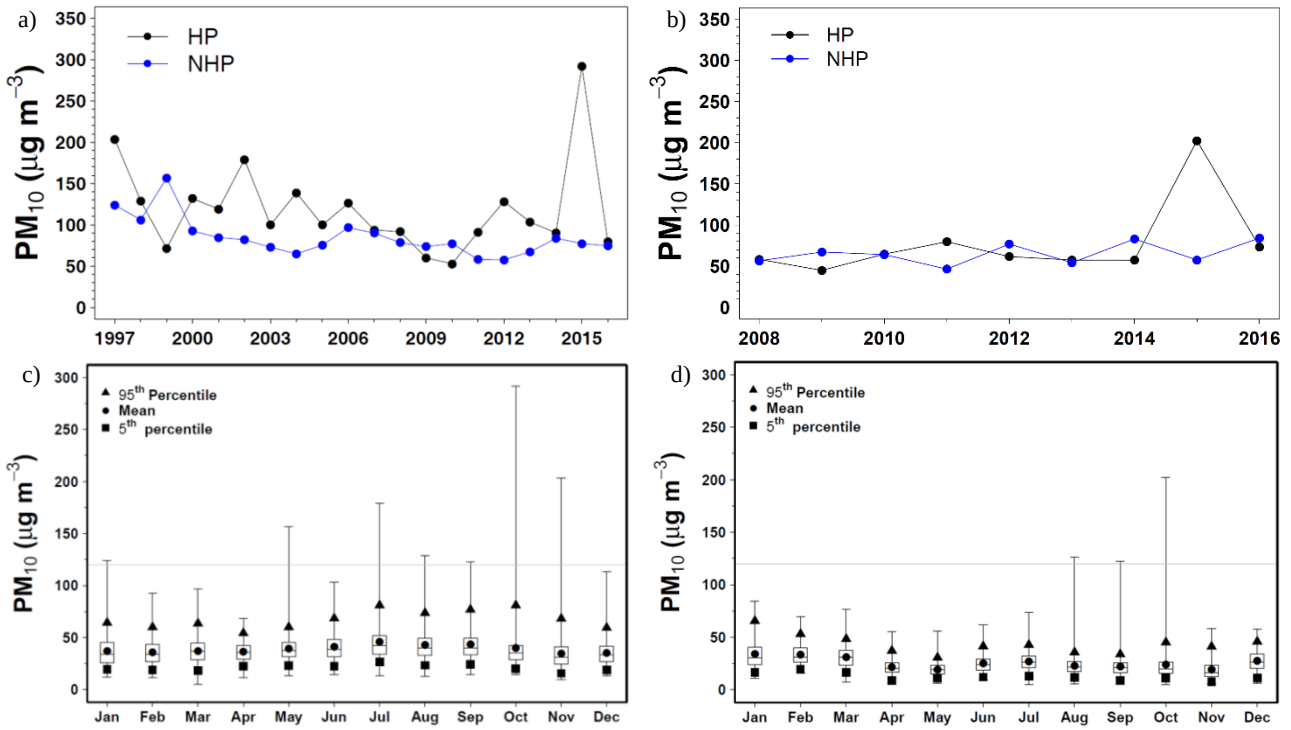


**Figure 5.** Annual maximum daily $PM_{10}$ at a) Songkhla and b) Phuket, and monthly $PM_{10}$ at c) Songkhla and d) Phuket. In a) and b), HP and NHP stand for the haze-prone and non-haze-prone periods, respectively. In each of the lower figures, the grey line indicates the national daily $PM_{10}$ standard. The bottom side, middle line, and top side of each box denote the 1st, 2nd (or median), and 3rd quartiles, respectively. The bottom and top dashes of each vertical line are the minimum and maximum of data.

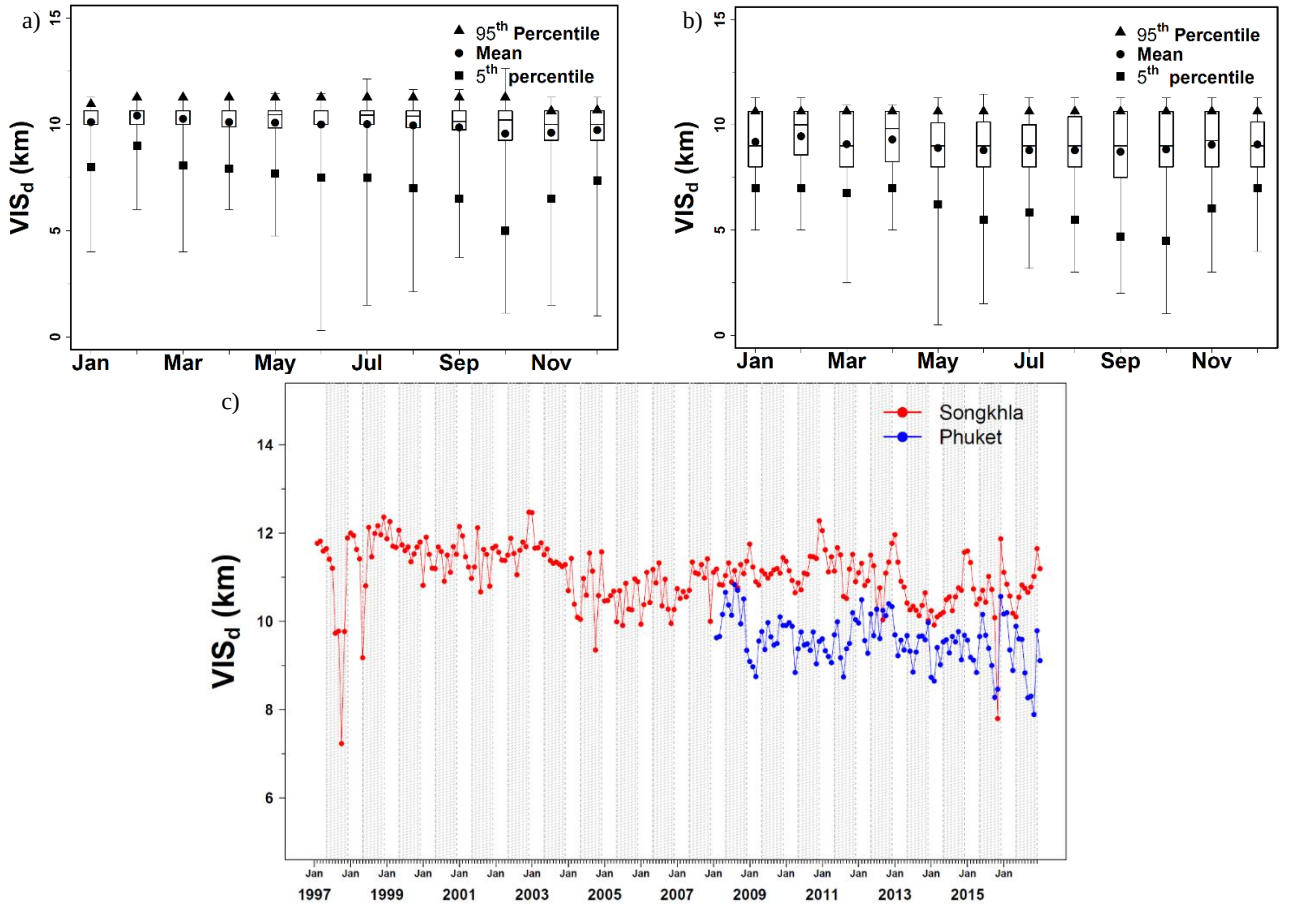


**Figure 6.** a) and b) Monthly $VIS_d$ at Songkhla and Phuket, respectively, and c) monthly variation of $VIS_d$ at both stations. The grey lines indecates the haze-prone months.

 

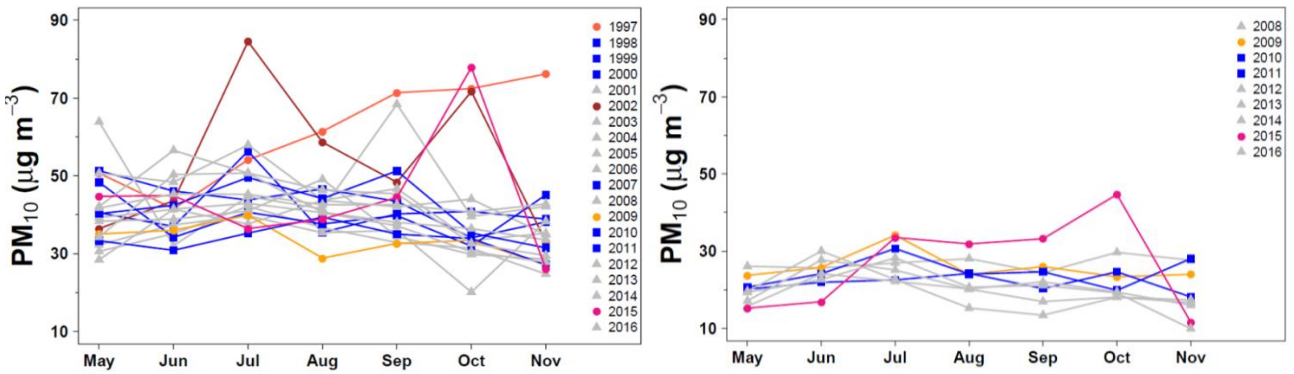


**Figure 7.** Monthly $PM_{10}$ in May-November at a) Songkhla and b) Phuket. The circles (in red, pink, orange, and yellow), blue squares, and grey triangles in the former figure denote the El Nino, La Nina, and neutral ENSO phases, respectively.

**4.2 $PM_{10}$ episodes and linkage to transboundary smoke haze**

As stated previously in Section 3, 42 elevated $PM_{10}$ episodes were identified at Songkhla based on 1997-2015 (Table 3). As much as 90% of all episodes are associated with El Nino (57%) or Neutral (i.e., the neutral phase) (33%). However, only 4 such episodes were found at Phuket based on 2008-2015, all of which were in the strong El Nino year 2015 (Table 4).

Figure 8 illustrates the simulated back-trajectory pathways in Episode No. 41 at Songkhla and Episode No. 3 at Phuket, representatively chosen given that both episodes fall within the same period (i.e., early October 2015) apparently with a subset of back-trajectories passing over Sumatra or Borneo. It is noted that October is generically in the transition of the southwest and northeast monsoons for Upper Southeast Asia. In the figure, the southwesterly and southwesterly winds dominate. The former winds bear the signature of the regional southwest monsoon whereas the latter winds are the trade winds moving northward to the monsoon trough (i.e., intertropical convergence zone).

a) Episode No. 41 at Songkhla

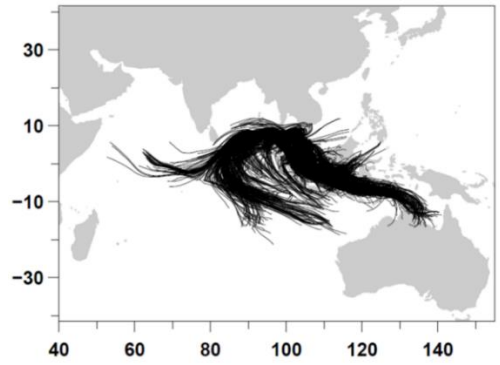


b) Episode No. 3 at Phuket

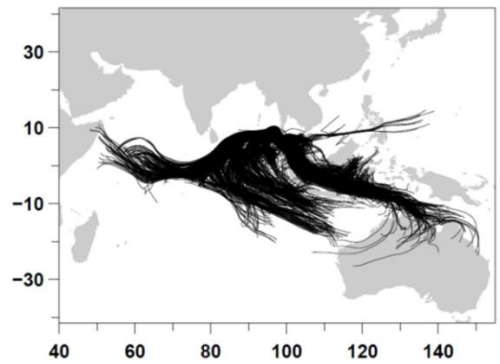


**Figure 8.** Back-trajectories for Songkhla Episode No. 41 at Songkhal and Episode No. 3 at Phuket. Each episode has a total of 1,512 trajectories.

Based on the back-trajectory results at Songkhla, the majority of the episodes (63%) have the simulated back-trajectories passing over fire cluster(s) located in Sumatra or Borneo. Out of 63%, 26% is of El Nino, 4% is of La Nina, and 33% is of Neutral. Thus, it is likely that El Nino and Neutral enhance the northward wind movement from Indonesia more than La Nina does. This suggestion is yet to be warranted through in-depth analysis in the future. Also notice from Tables 3 that several episodes in the El Nino years 2002 and 2015 had relatively high percentage values (>50%) of back-trajectories passing over Sumatra or Borneo, in agreement with the relatively large numbers of fires found (Figure 9).

a) Sumatra

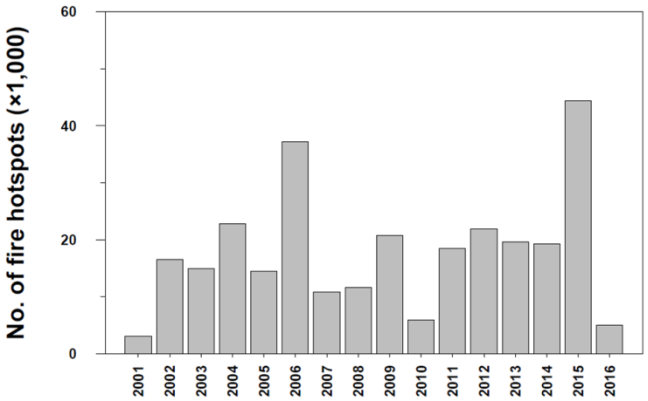


b) Borneo

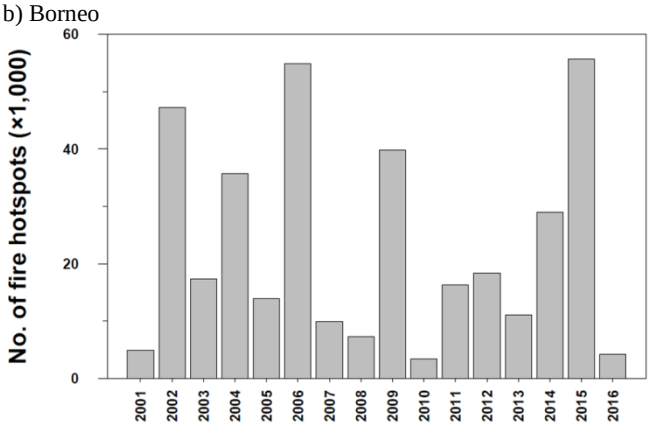


**Figure 9.** Annual total MODIS fire hotspots during the haze-prone period during 2001-2016 over Sumatra (top) and Borneo (bottom). Note that the year 2001 has the fire hotspot data from Terra only whereas the other years have those from both Terra and Aqua combined.

Similarly, the El Nino year 2009 also had fires being well present but without elevated $PM_{10}$ episodes or high $PM_{10}$ levels at both Songkhla and Phuket (Figure 7). This may be partly explained by the timings of fire occurrence and favorable wind pattern not concurring or matching to promote the smoke haze migration to the southern region of Thailand.

Also notice that about one third of all elevated $PM_{10}$ episodes at Songkhla do not have the presence of fires matched with back-trajectories (Table 3). This is possibly attributed by a number of limitations or factors, e.g., the capability of satellite fire detection, the applied back-trajectory method which uses only wind fields to drive simulation without other complex physical processes (such as turbulent dispersion and wet removal or scavenging by precipitation), the coarse grid resolution of the driving wind fields, and no background smoke haze already existing in the atmosphere taken into account in our modeling.

## 5. Conclusions

The long-term air quality was used to investigate the extent and impact of transboundary haze from Indonesia on air quality in Southern Thailand. The focus was given to the two major provinces in the region, which are Songkhla and Phuket as the representative study areas in the eastern- and western-coast sides of the region. Elevated $PM_{10}$ tends to occur in the haze-prone period and be more induced in the relatively strong El Nino years (here, 1997 and 2015). $PM_{10}$ degradation at Songkhla was the most pronounced among Phuket and the other three provinces considered. The seasonality of monthly mean $PM_{10}$ and $VIS_d$ is not as apparent as that of the high-end and low-end percentiles respectively, suggesting a high degree of episodicity for the smoke haze problem. The results of kinematic back-trajectories simulated for each identified elevated $PM_{10}$ episode (42 and 4 episodes at Songkhla and Phuket, respectively) show that the majority of the episodes (63% at Songkhla and 100% at Phuket) have the simulated back-trajectories passing over fire cluster(s) located in Sumatra or Borneo and often associated with the warm (El Nino) or neutral phases of ENSO. This result affirms the potential migration of transboundary smoke haze, as multi-country attention and cooperation has long been called for to understand and deal with biomass burning in Indonesia and the associated transboundary smoke haze issue.

A number of technical limitations in the current study are acknowledged. Firstly, only simple back-trajectory modeling was utilized using coarse-grid wind fields, which does not consider local and regional emissions, complex physical atmospheric processes, and the background condition of pollution. It is known that atmospheric fine particles can also form by gaseous precursors, needing an integrated or advanced air quality modeling technique to account for. Our simple matching between back-trajectory pathways to fire clusters, which is the case here, only gives a general evidence of linking smoke haze to biomass burning. Other trajectory-based statistical methods, such as concentration field (CF) and potential source contribution function (PSCF) [23, 28], can enhance the source-receptor linkage more objectively. Importantly, robust source identification or attribution generally requires comprehensive emission inventories to be incorporated, which were not included here but necessary in addressing how particulate matter comes from (local, regional, and transboundary). Moreover, scientific insight into the synoptic or regional weather systems in context of transboundary smoke haze is of interest and needed to help clarify how smoke haze is migrated northward from Indonesia to other countries. Given that $PM_{2.5}$ (particulate matter whose size is 2.5 μm or smaller) may be used as a better representation of fine particulate matter (here, transboundary smoke haze) than $PM_{10}$, future studies should pay attention to $PM_{2.5}$ for which the PCD have extended the routine operational monitoring at many stations in the southern region in very recent years.

## Acknowledgements

The authors sincerely thank the Pollution Control Department and the Thai Meteorological Department for the observational data. This study was financially supported mainly by The Joint Graduate School of Energy and Environment (JGSEE), King Mongkut's University of Technology Thonburi and the Center of Excellence on Energy Technology and Environment (CEE), PERDO, Ministry of Higher Education, Science, Research and Innovation, and the Postgraduate Education and Research Development Office, and partly by the National Research Council of Thailand and the Hydro Informatics Institute (Public Organization).

## References

[1] Streets, D.G., Yarber, K.F., Woo, J.H. and Carmichael, G.R. 2003. Biomass burning in Asia: Annual and seasonal estimates and atmospheric emissions, *Global Biogeochemical Cycles*, 17, 1099, doi:10.1029/2003GB002040.

[2] Field, R.D., Van Der Werf, G.R. and Shen, S.S. 2009. Human amplification of drought-induced biomass burning in Indonesia since 1960, *Nature Geoscience*, 2, 185. doi:10.1038/ngeo443.

[3] Hao, W.M. and Liu, M.H. 1994. Spatial and temporal distribution of tropical biomass burning, *Global Biogeochemical Cycles*, 8, 495-503.

[4] Vadrevu, K.P., Lasko, K., Giglio, L., Schroeder, W., Biswas, S. and Justice, C. 2019. Trends in vegetation fires in South and Southeast Asian countries, *Scientific Reports*, 9, 7422, doi:10.1038/s41598-019-43940-x.

[5] Field, R.D., Spessa, A.C., Aziz, N.A., Camia, A., Cantin, A., Carr, R., de Groot, W.J., Dowdy, A.J., Flannigan, M.D., Manomaiphiboon, K., Pappenberger, F., Tanpipat, V. and Wang, X. 2015. Development of a global fire weather database, *Natural Hazards and Earth System Sciences*, 15, 1407-1423.

[6] Page, S.E. and Hooijer, A. 2016. In the line of fire: the peatlands of Southeast Asia, *Philosophical Transactions of the Royal Society B: Biological Sciences*, 371, 20150176. 10.1098/rstb.2015.0176.

[7] Aouizerats, B., Van Der Werf, G.R., Balasubramanian, R. and Betha, R. 2015. Importance of transboundary transport of biomass burning emissions to regional air quality in Southeast Asia during a high fire event, *Atmospheric Chemistry and Physics*, 15, 363-373.

[8] Pentamwa, P. and Oanh, N.T.K. 2008. Air quality in Southern Thailand during haze episode in relation to air mass trajectory, *Songklanakarin Journal of Science & Technology*, 30, 539-546.

[9] Reddington, C.L., Yoshioka, M., Balasubramanian, R., Ridley, D., Toh, Y.Y., Arnold, S.R. and Spracklen, D.V. 2014. Contribution of vegetation and peat fires to particulate air pollution in Southeast Asia, *Environmental Research Letters*, 9, 223-237.

[10] Wipatayotin, A. 2019. South put on haze alert. Bangkok Post, Available online: https://www.bangkokpost.com/thailand/general/1753869/south-put-on-haze-alert [Accessed: 24 October 2019].

[11] Aldrian, E. and Susanto, R.D. 2003. Identification of three dominant rainfall regions within Indonesia and their relationship to sea surface temperature, *International Journal of Climatology*, 23, 1435-1452.

 

[12] Fuller, D.O. and Murphy, K. 2006. The ENSO fire dynamic in insular Southeast Asia, *Climatic Change*, 74, 435-455.
[13] Chan, L.Y., Chan, C.Y., Liu, H.Y., Christopher, S., Oltmans, S.J. and Harris, J.M. 2000. A case study on the biomass burning in Southeast Asia and enhancement of tropospheric ozone over Hong Kong, *Geophysical Research Letters*, 27, 1479-1482.
[14] Dotse, S.Q., Dagar, L., Petra, M.I. and De Silva, L.C. 2016. Influence of Southeast Asian Haze episodes on high $PM_{10}$ concentrations across Brunei Darussalam, *Environmental Pollution*, 219, 337-352.
[15] PCD. 2016. *Thailand State of Pollution Report 2015*, Pollution Control Department, Thailand, Available online: http://infofile.pcd.go.th/mgt/Report_Eng2553.pdf?CFID=13602443&CFTOKEN=48440808 [Accessed: 10 April 2017].
[16] Torsri, K., Octaviani, M., Manomaiphiboon, K. and Towprayoon, S. 2012. Regional mean and variability characteristics of temperature and precipitation over Thailand in 1961-2000 by a regional climate model and their evaluation, *Theoretical and Applied Climatology*, 113, 289-304.
[17] TMD. 2017. *Climate of Thailand*, Thai Meteorological Department, Thailand, Available online: https://www.tmd.go.th/en/archive/thailand_climate.pdf [Accessed: 20 June 2017].
[18] Seinfeld, J.H. and Pandis, S.N. 2016. *Atmospheric chemistry and physics: from air pollution to climate change*, John Wiley & Sons.
[19] Rosenfeld, D., Dai, J., Yu, X., Yao, Z., Xu, X., Yang, X. and Du, C. 2007. Inverse relations between amounts of air pollution and orographic precipitation, *Science*, 315, 1396-1398.
[20] Aman, N., Manomaiphiboon, K., Pengchai, P., Suwanathada, P., Srichawanae, J. and Assareh, N. 2019. Long-term observed visibility in Eastern Thailand: temporal variation, association with air pollutants and meteorological factors, and trends, *Atmosphere*, 10, 122, doi:10.3390/atmos10030122.
[21] Stohl, A., Wotawa, G., Seibert, P. and Kromp-Kolb, H. 1995. Interpolation errors in wind fields as a function of spatial and temporal resolution and their impact on different types of kinematic trajectories, *Journal of Applied Meteorology*, 34, 2149-2165.
[22] Saha, S., Moorthi, S., Pan, H.L., Wu, X., Wang, J., Nadiga, S., Tripp, P., Kistler, R., Woollen, J., Behringer, D., Liu, H., Stokes, D., Grumbine, R., Gayno, G., Wang, J., Hou, Y.T., Chuang, H.-Y., Juang, H.-M.H., Sela, J., Iredell, M., Treadon, R., Kleist, D., Delst, P.V., Keyser, D., Derber, J., Ek, M., Meng, J., Wei, H., Yang, R., Lord, S., Dool, H.V.D., Kumar, A., Wang, W., Long, C., Chelliah, M., Xue, Y., Huang, B., Schemm, J.-K., Ebisuzaki, W., Lin, R., Xie, P., Chen, M., Zhou, S., Higgins, W., Zou, C.-Z., Liu, Q., Chen, Y., Han, Y., Cucurull, L., Reynolds, R.W., Rutledge, G. and Goldberg, M. 2010. The NCEP Climate Forecast System, *Bulletin of the American Meteorological Society*, 315, 1015-1057.
[23] Begum, B.A., Kim, E., Jeong, C.H., Lee, D.W. and Hopke, P.K. 2005. Evaluation of the potential source contribution function using the 2002 Quebec forest fire episode, *Atmospheric Environment*, 39, 3719-3724.
[24] Fleming, Z.L., Monks, P.S. and Manning, A.J. 2012. Untangling the influence of air-mass history in interpreting observed atmospheric composition, *Atmospheric Research*, 104-105, 1-39.
[25] Potier, E., Waked, A., Bourin, A., Minvielle, F., Péré, J.C., Perdrix, E., Michoud, V., Riffault, V., Alleman, L.Y. and Sauvage, S. 2019. Characterizing the regional contribution to $PM_{10}$ pollution over northern France using two complementary approaches: Chemistry transport and trajectory-based receptor models, *Atmospheric Research*, 223, 1-14.
[26] Wotawa, G., Kröger, H. and Stohl, A. 2000. Transport of ozone towards the Alps–results from trajectory analyses and photochemical model studies, *Atmospheric Environment*, 34, 1367-1377.
[27] Giglio, L. 2010. *MODIS collection 5 active fire product user's guide version 2.4*, Science Systems and Applications, Inc.
[28] Stohl, A. 1998. Computation, accuracy and applications of trajectories a review and bibliography, *Atmospheric Environment*, 32, 947-966.

 